Journal of the Korean Nuclear Society
Volume 17, Number 4, December 1985

The Analysis of Stability in a Steam Generator

Shin Whan Kim and Goon Cherl Park

Seoul National University

(Received July 24, 1985)

증기발생기의 안정성 분석

김 신 환·박 군 철

서울대학교

(1985. 7. 24 접수)

Abstract

The purpose of this paper is to investigate the density-wave oscillation type instability in the recirculating loop of U-tube steam generator (UTSG). The perturbed and nodalized conservations equations based on the drift-flux model have been derived to obtain the single-and two-phase pressure drop perturbations, by taking into account the slip between phases, nonuniform heat flux and heated wall dynamics. To assess the stability, the frequency domain technique with the Nyquist criterion has been used under the constant pressure drop boundary condition throngh the loop.

The computer implementation of this model, SASG, was used for the parametric study of the steam generator in Kori-Unit 1. The results of the parametric study revealed important factors influencing UTSG stability margin.

요 약

U-tube 증기발생기 내부의 재순환 loop에서의 밀도파 진동 형태의 불안정성 분석을 하고저 한다.

단상과 2상 영역에서의 압력 강하의 섭동치를 계산하기 위하여, 상간의 slip과 비균일 열유랑 그리고 heated wall dynamics를 고려하여 drift-flux model에 근거를 둔 노드 내의 섭동 보존 방정식이 유도되었다. Loop를 통한 일정 압력강하 경계조건하에 Nyquist 조건을 사용하여 안정성이 분석되었다.

SASG computer program을 개발하여 고리 1호기의 증기 발생기에 대한 안정성을 분석하였으며, 아울러, 중요한 계통인자들의 안정성 여유도에 미치는 영향도 분석하였다.

Nomeclature

A	flow area (ft²)
C_0	void concentration parameter
C_K	kinematic wave velocity (ft/s)
c_P	specific heat at consant pressure (Btu/lb F)
D_H	hydraulic diameter (ft)
f	Darcy-Weisbach frication factor
G	flow mass flux (lb/hr-ft²)
g	acceleration of gravity (32.174 ft/sec²)
g_c	conversion factor (32.174 lb-ft/lbf-sec²)
h	enthalpy (Btu/lb)
H	heat transfer coefficient (Btu/hr-ft²-F)

j_i heated section inlet velocity (ft/s)
K local loss coefficient
k thermal conductivity (Btu/ft-F-s)
L total number of single-phase nodes in the heated section
K_H heated section length (ft)
M total number of spacers
N total number of nodes in the heated section
p pressure (psia)
P_H heated perimeter (ft)
q'' heat flux (Btu/ft^2-s)
s $j\omega$ where ω is frequency (rad/s)
T temperature (F)
V_{gj} drift-velocity (ft/s)
W mass flow rate (lb/hr)
$\langle x \rangle$ cross-sectional averaged flow quality
z axial position (ft)
Δz axial length of the node (ft)
α thermal diffusivity (ft^2/s)
$\langle \alpha \rangle$ cross-sectional averaged void fraction
ϕ_{lo}^2 two-phase friction loss multiplier
Φ two-phase local loss multiplier
ρ density (lb/ft^3)
Ω characteristic frequency of phase change (s^{-1})
λ boiling boundary (ft)
$\langle \phi \rangle$ cross-sectional average of parameter ϕ
$\delta\hat{\phi}$ perturbed and Laplace-transformed ϕ

Superscript/Subscript

1ϕ single-phase
2ϕ two-phase
B inlet boundary node index of the two-phase region
DC downcomer
f saturated liquid
g saturated vapor
fw feed water
P primary side
R riser
s secondary side
sw saturated water
w heater wall

I. Introduction

Flow instabilities during the boiling process can produce unfavourable conditions in a system. A classification and description of the characteristics, parametric effects and physical mechanisms of the various types of flow instability have been presented previously.[1],[2]

The most common instability which is encountered in practice is the density-wave oscillation type instability.[3] This is due to multiple regenerative feedbacks between mass flow rate, vapor generation rate and pressure drop. This type of flow instablity can occur in closed loop systems such as UTSG secondary side recirculation loop which is composed of a heated section, a riser including the steam separator and a downcomer.

The purpose of this study is to develope a state-of-the-art one dimensional thermal-hydraulic model which can be used for the linear analysis of the density-wave instability in the UTSG recirculation loop. The resultant accounts for slip between phases, local friction, nonuniform heat flux, and distributed heated wall dynamics.

The recirculation loop in UTSG is divided into three regions; the heated section, the adiabatic riser and the downcomer, in which the pressure drop perturbations are calculated by solving the linearized and Laplace-transformed conservation equations with the following assumptions;

1) The system pressure is constant,
2) The flow in the channel is treated as one dimensional by using the cross-sectional averaged quantities,
3) Potential and kinetic energy terms are ignored in comparision with thermal energy term.

4) There are negligible internal heat generation and heat conduction in the fluid,
5) The thermal properties of the heater are assumed to be constant,
6) Subcooled boiling is neglected.

In heated section region a nodal approximation of the conservation equation is used. Thus the axial nonuniform heat flux distribution is replaced by a stepwise uniform function such that the linearized, Laplace-transformed governing equations can be integrated analytically over the node. The resultant nodal pressure drop perturbations are summed and applied to the constant pressure drop boundary condition through the loop, i.e.

$$\delta(\Delta P_{1\phi})_{loop}+\delta(\Delta P_{2\phi})_{loop}=0,$$

in order to yield the open-loop transfer function for the stability analysis based on the Nyquist criterion.

The computer implementation of this model, SASG was used for the parametric study of UTSG in Kori-Unit 1.

II. Modeling

In this study, the recirculation loop is modeled as shown in Figure 2.1. The loop is divided into three regions; the heated section, the adiabatic riser and the downcomer.[4],[5] To assess the stability analysis, the pressure drop perturbations in each region are treated separately. In the heated section a nodal approximation is used, and the other regions are treated as one volume.

The following sections describe the steady state parameter calculation and, then, pressure drop perturbations in each region.

II. 1. Steady-State Primary-to-Secondary Heat Flux

In the analysis of flow instablitiy it is very important to know the steady-state operating conditions since they provide initial conditions to the calculation. Among these steady-state conditions, the primary-to-secondary heat flux plays very important role in the analysis.

To find the steady state heat flux, the heated section region is nodalized such that the secondary side is divided into N nodes, and for each node there are two corresponding primary nodes, one for up-flow and the other for down-flow. In each set of nodes the heat flux is calculated from the energy balance on the assumption of constant system pressure and with the inlet boundary conditions.

For the i-th node the calculation procedure is

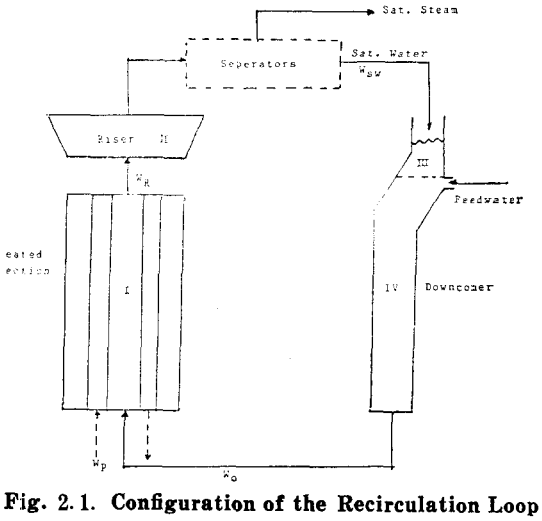

Fig. 2.1. Configuration of the Recirculation Loop

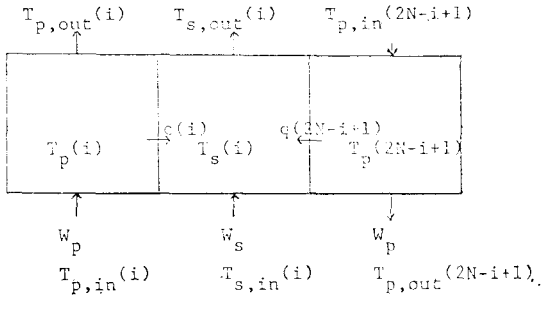

The average temperatures in each node are defined as,

$$T_p(i)=(T_{p,in}(i)+T_{p,out}(i))/2. \quad (2.1)$$

$$T_s(i)=(T_{s,in}(i)+T_{s,out}(i))/2. \quad (2.2)$$

$$T_p(2N-i+1)=(T_{p,in}(2N-i+1)+T_{p,out}(2N-i+1))/2. \quad (2.3)$$

based on the following diagram.

And heat transfered to the secondary side is given by

$$q(i)=A_iU(i)[T_p(i)-T_s(i)] \quad (2.4)$$

$$q(2N-i+1)=A_iU(2N-i+1)[T_p(2N-i+1)-T_s(i)] \quad (2.5)$$

Then, from the steady state energy balance node inlet and outlet temperatures are calculated as

$$T_{p,\mathrm{out}}(i)=T_{p,\mathrm{in}}(i)-\frac{q(i)}{W_pC_{pp}} \quad (2.6)$$

$$T_{s,\mathrm{out}}(i)=T_{s,\mathrm{in}}(i)-\frac{q(i)+q(2N-i+1)}{W_sC_{ps}} \quad (2.7)$$

$$T_{p,\mathrm{in}}(2N-i+1)=T_{p,\mathrm{out}}(2N-i+1)+\frac{q(2N-i+1)}{W_pC_{pp}} \quad (2.8)$$

For circular tube, the overall heat transfer coefficients in Equation (2.4) and (2.5) are defined in terms of the outside area of the tube as[6]

$$U=\frac{1}{\frac{A_0}{A_ih_i}+\frac{A_0ln(r_0/r_i)}{2\pi kL}+\frac{1}{h_0}}$$

In this calculation the single-phase heat transfer coefficients are calculated from Dittus-Boelter correlation[1] and the two-phase heat transfer coefficients are calculated from Thom's correlation.[1]

Equations from (2.1) to (2.8) are iterated with the known values of $T_{p,\mathrm{in}}(i)$ and $T_{s,\mathrm{in}}(i)$ and $T_{p,\mathrm{out}}$ $(2N-i+1)$ until the node average temperatures converge to some value.

When, for some node, the secondary node outlet temperature is greater than the saturation temperature, the boiling boundary is calculated by interpolation. Then, after that node, two-phase region begins and both phases are assumed to be at saturation temperature.

This calculation is carried out node by node to the last node, and the primary-to-secoudary heat flux of the i-th node can be obtained by summing the resultant heat flux in the i-th node and the $(2N-i+1)$-th node.

II. 2 The Drift-Flux Model

In this study a nodal approximation is used, in which the axial heat flux distribution is replaced by a piecewise constant function. Nonlinearities in the two-phase conservation equations are removed through a first order perturbation expansion. Then the resultant equations are Laplace-transformed to convert the analysis of system dynamics from the time domain to the frequency domain.

The final forms of the nodal perturbed and Laplace-transformed conservation equations are given under the assumptions in Section I for the k-th node as;

(1) Nodal mixture continuity equation

$$\frac{d\delta\langle\hat{j}\rangle_k}{dz}=\delta\hat{Q}_k \quad (2.9)$$

(2) Nodal momentum equation

$$\frac{d}{dz}\delta(\Delta\hat{P}_{2\phi})_k=\frac{1}{g_c}\left(s\delta\hat{G}+\frac{d\delta\hat{G}'}{dz}\right)+\frac{fG_0\phi_{l0}^2}{g_c\rho_fD_H}\delta\hat{G}+\frac{fC_0^2}{2g_c\rho_fD_H}\delta\hat{\phi}_{l0}^2+\frac{g}{g_c}\delta\langle\hat{\rho}\rangle$$
$$+\frac{d}{dz}\delta\left\{\left(\frac{\rho_f-\langle\rho\rangle}{\langle\rho\rangle-\rho_g}\right)\frac{\rho_f\rho_g}{\langle\rho\rangle}\overline{(V'_{gj})^2}\right\}+\sum_{m=1}^{M}K_{\mathrm{spacer},m}\left\{\frac{G_0\Phi_0}{g_c\rho_f}\Big|_{z=z_m}\delta\hat{G}(s,z_m)\right.$$
$$\left.+\frac{G_0^2}{2g_c\rho_f}\Big|_{z=z_m}\delta\hat{\Phi}(s,z_m)\right\}+K_{\mathrm{exit}}\left\{\frac{G_0\Phi_0}{g_c\rho_f}\Big|_{z=L_H}\delta\hat{G}(s,L_H)+\frac{G_0^2}{2g_c\rho_f}\Big|_{z=L_H}\delta\hat{\Phi}(s,z_m)\right\} \quad (2.10)$$

(3) Nodal conduction equation

$$\nabla^2\delta\hat{T}_k-\frac{s}{\alpha}\delta\hat{T}_k+\frac{1}{k}\delta\hat{q}_k'''=0 \quad (2.11)$$

(4) Nodal void propagation equation

$$s\delta\langle\hat{\alpha}\rangle_k+\frac{d\langle\alpha_0\rangle_k}{dz}\delta(\hat{C}_K)_k+(C_{K,0})\frac{d\delta\langle\hat{\alpha}\rangle_k}{dz}=\left(\frac{\rho_f}{\Delta_\rho}-C_0\langle\alpha_0\rangle_k\right)\delta\hat{\Omega}_k-C_0\Omega_{0,k}\delta\langle\hat{\alpha}\rangle_k \quad (2.12)$$

II. 3. Heated Wall Dynamics

Heated wall dynamics is important in the stability analysis. In the single-phase region, it affects the boiling boundary dynamics and thus introduces a lag between the inlet flow perturbation and the void fraction perturbations in the two-phase region. In the two-phase region it also plays an important role because of the time lag between the heat flux perturbations and the void fraction perturbations.

In this study, a distributed parmeter model for a cylindrical tube is developed. For a cylindrical tube, Equa tion (2.11), with neglecting the internal heat generation in the tube wall, becomes

$$\frac{1}{r}\frac{d}{dr}\left(r\frac{d\delta\hat{T}}{dr}\right)-\frac{s}{\alpha}\delta\hat{T}=0 \quad (2.13)$$

Integrating Equation (2.13) with the perturbed boundary conditions,

$$-k\frac{d\delta\hat{T}}{dr}\Big|_{r=r_i}=\delta\hat{q}_p'''$$

$$-k\frac{d\delta\hat{T}}{dr}\Big|_{r=r_0}=\delta\hat{q}_s''$$

then, the heater wall temperature perturbation $r=r_0$ becomes

$$\delta\hat{T}_w=Z_{1c}(s)\delta\hat{q}_s''+Z_{2c}(s)\delta\hat{q}_p'' \quad (2.14)$$

where,

$$Z_{1c}(s)=\frac{1}{k\varepsilon\theta}\{I_0(\varepsilon r_0)K_1(\varepsilon r_i)+I_1(\varepsilon r_i)K_0(\varepsilon r_0)\}$$

$$Z_{2c}(s)=\frac{-1}{k\varepsilon\theta}\{I_0(\varepsilon r_0)K_1(\varepsilon r_0)+I_1(\varepsilon r_0)K_0(\varepsilon r_0)\}$$

$$\theta=I_1(\varepsilon r_i)K_1(\varepsilon r_0)-I_1(\varepsilon r_0)K_1(\varepsilon r_i)$$

$$\varepsilon=\sqrt{s/\alpha}$$

In order to express $\delta\hat{q}_s''$ in terms of the forcing functions, $\delta\hat{j}_i$ and $\delta\hat{q}_p''$, $\delta\hat{T}_w$ can be eliminated from Equation (2.14) by using the Newton's law of cooling.

For the single-phase region,

$$q''=H_{\phi 1}(T_w-T_\infty). \quad (2.15)$$

By perturbing and Laplace transforming,

$$\frac{\delta\hat{q}_s''}{q_{0s}''}=a\frac{\delta j_i}{j_{i0}}+\frac{H_{1\phi 0}}{q_{0s}}(\delta\hat{T}_w-\delta\hat{T}_\infty) \quad (2.16)$$

where, a is Reynolds number exponent.

Using the heated wall dynamics model,

$$\frac{\delta\hat{q}_s''}{q_{0s}''}=\frac{1}{(1-H_{1\phi}Z_{1c}(s))}\,a\frac{\delta\hat{j}_i}{j_{io}}+H_{1\phi}Z_{2c}(s)\frac{\delta\hat{q}_p''}{q_{0s}''} \quad (2.17)$$

In the two-phase region, the heat transfer equation has the form of

$$q''=\chi(T_w-T_{sat})^m \quad (2.18)$$

where, $\chi$and m are empirical constants. By perturbing and Laplace-transforming, and using the heated wall dynamics, the final form of $\delta\hat{q}_s''$ in the two-phase region becomes

$$\delta\hat{q}_s''=Z_{3c}(s)\delta\hat{q}_p'' \quad (2.19)$$

where,

$$Z_{3c}(s)=\frac{\kappa Z_{2c}(s)}{1-Z_{1c}(s)},\ \text{and}$$

$$\kappa=m\chi(T_{w0}-T_{sat})^{m-1}$$

II. 4. Final Forms of The Thermal-Hydraulic Transfer Functions

In the stability analysis, the pressure drop perturbations are subject to the boundary condition,

$$\delta(\Delta\hat{P}_{1\phi})_{loop}+\delta(\Delta\hat{P}_{2\phi})_{loop}=0 \quad (2.20)$$

In this analysis, the pressure drop peturbations in each three regions of the recirculating loop are calculated separately. Then, inserting these perturbations into Equation (2.20), the final transfer function can be obtained.

II. 4. 1. Heated Section

The heated section will be splited by the boiling boundary to the single-and two-phase region. For the single-phase region, the perturbed and Laplace-transformed momentum equation is integrated from the inlet to the moving boiling boundary by using Leibniz's rule, and expressed in terms of the external forcing functions, as,

$$\delta(\Delta P_{1\phi})=\Gamma_1(s)\delta\hat{j}_i+\sum_{k=1}^{L}\Gamma_{2,k}(s)\delta q''_{p,k} \quad (2.21)$$

where,

$$\Gamma_1(s)=\left(\frac{\rho_f}{g_c}s-+\frac{f\rho_f j_{i0}}{g_c D_H}\right)\lambda_0 + \left(\sum_{m=1}^{MS} K_{\text{spacer}}\right)\frac{G_0}{g_c}+C_2\Lambda_1(s)$$

$$\Gamma_{2,k}(s)=\left(\frac{fG_0^2}{2g_c D_H\rho_f}+\frac{g}{g_c}\rho_f\right)\Lambda_2(s)H_k'(s)$$

In this calculation the boiling boundary perturbation is obtained from

$$\delta\hat{\lambda}=\frac{-\delta\hat{h}(s,\lambda_0)}{\left.\frac{dh}{dz}\right|_{z=\lambda_0}} =\Lambda_1(s)\delta\hat{j}_i+\Lambda_2(s)\sum_{k=1}^{L}H_k'(s)\delta\hat{q}_{p,k}'' \quad (2.22)$$

where, the terms $\delta\hat{h}$and $(dh/dz)\,|_{z=\lambda_0}$ can be calculated from the perturbed and the steady-state single phase energy equations, respectively.

In order to obtain the two-phase pressure drop perturbation, $\delta(\Delta\hat{P}_{2\phi})$, the perturbed mixture momentum equation should be integrated node by node and summed up over all the nodes in the two-phase region. To make the nodal integration simple, the coordinate, z_k, is transformed to ξ_k defined as,

$$\xi_k(z_k)=(C_{k,0}(z))_k/(C_{K,0})_k^{\text{in}} \quad (2.23)$$

Then, for the k-th node except for the inlet node having the moving boundary, $\delta(\Delta\hat{P}_{2\phi})_k$ comes from the integration of Equation (2.10) as (exclusive of local loss),

$$\delta(\Delta\hat{P}_{2\phi})_k=\frac{(C_{k,0})_k^{\text{in}}}{C_0\Omega_0}\int_1^{\xi_{0,k}^{\text{out}}}\left[\frac{1}{g_c}\left(s\delta\hat{G}+\frac{C_0\Omega_{0,k}}{(C_{k,0})_k^{\text{in}}}\frac{d\delta\hat{G}'}{d\xi_{0,k}}\right)+\frac{fG_0\phi_{10}^2}{g_c\rho_f D_H}\delta\hat{G}+\frac{fG_0^2}{2g_c\rho_f D_H}\delta\hat{\phi}_{10}^2 + \frac{g}{g_c}\delta\langle\hat{\rho}\rangle+\frac{1}{g_c}\frac{C_0\Omega_{0,k}}{(C_{k,0})_k^{\text{in}}}\frac{d}{d\xi_{0,k}}\delta\overline{\left\{\left(\frac{\rho_f-\langle\rho\rangle}{\langle\rho\rangle-\rho_g}\right)\frac{f_g}{\langle\rho\rangle}(V_{gj}')^2\right\}}\right]d\xi_{0,k} + K_{\text{loss}}\left\{\left.\frac{G_0\Phi_0}{g_c\rho_f}\right|_{z=z_m}\delta\hat{G}(s,z_m)+\frac{G_0^2}{2g_c\rho_f}\delta\Phi(s,z_m)\right\} \quad (2.24)$$

And the local pressure drop perturbation due to spacers located at z_m and a loss at the channel exit is given by,

$$\delta\{\Delta\hat{P}_{\text{loss}}(z_m)\}=K_{\text{loss}}\left\{\left.\frac{G_0\Phi_0}{g_c\rho_f}\right|_{z=zm}\delta\hat{G}(s,z_m) + \frac{G_0^2}{2g_c\rho_f}\delta\hat{\phi}(s,z_m)\right\} \quad (2.25)$$

In this calculation, the density perturbation, $\delta\langle\hat{p}\rangle$, and the mixture mass flux perturbation, $\delta\hat{G}$, can be obtained from solving the perturbed density propagation equation and the corresponding correlation, [1]

$$G=\{\rho_f-\Delta\rho C_0\langle\alpha\rangle\}\langle j\rangle-\Delta\rho V_{gj}\langle\alpha\rangle, \quad (2.26)$$

respectively. The two-phase friction loss coefficient perturbation, $\delta\hat{\Phi}_{10}^2$, is also obtained from perturbing the general expression for this parameter,

$$\phi_{10}^2=\{C_2+C_1\frac{v_{fg}}{v_f}\langle x\rangle\} \quad (2.27)$$

where C_1 and C_2 are empirical parameters, which are both unity for homogeneous flow. In this study, as an option, C_1 and C_2 are fitted to the Martinelli-Nelon model. And the quality perturbation can be calculated from perturbing the Zuber-Findley void-quality correlation and by inserting the void fration perturbation which is directly related to the density perturbation.

For the inlet node of the two-phase region, the effect of the boiling boundary movement should be taken into account as,

$$\delta(\Delta\hat{P}_{2\phi})_B=\int_{\lambda(t)}^{z_B}-\left(\frac{d\delta\hat{p}}{dz}\right)dz =\int_{\lambda_0}^{z_B}\frac{d\delta p}{dz}dz-\left(\frac{dp}{dz}\right)_{z=\lambda_0}\delta\hat{\lambda} \quad (2.28)$$

Thus the total two-phase pressure drop perturbation can be obtained by summing all $\delta(\Delta\hat{P}_{2\phi})_k$ given in Equations (2.24) and (2.28) including $\delta\{\Delta\hat{P}_{\text{loss}}(z_m)\}$ given in Equation (2.25), and expessed in terms of the external forcing functions as the form of

$$\delta(\Delta\hat{p}_{2\phi})=\Pi_1(s)\delta\hat{j}_i+\sum_{k=1}^{K}\Pi_2^k(s)\delta\hat{q}_p'' \quad (2.29)$$

II. 4. 2. Riser

In this study, the riser region is assumed to

be adiabatic, and the flow in this region is assumed to be homogeneous since the flow area is large and thus the mixing is quite good.

The pressure drop perturbation across the riser can be calculated from the perturbed mixture momentum equation. Due to the large cross-sectional flow area and mixing, the hydrostatic head makes the dominant contribution to the pressure drop excluding the local losses due to the flow area change. Then, the perturbed momentum equation becomes

$$\delta(\Delta\hat{P}_R)=\frac{g}{g_c}\int_{L_H}^{L_R}\delta\langle\hat{\rho}\rangle dz + K_{\text{inlet},R}\left\{\frac{G_{R0}\Phi_R}{g_c\rho_f}\Big|_{L_H}\delta\hat{G}(s,L_H) + \frac{G_{R0}^2}{2g_c\rho_f}\Big|_{L_H}\delta\hat{\Phi}_R(L_H)\right\} + K_{\text{exit},R}\left\{\frac{G_{R0}\Phi_R}{g_c\rho_f}\Big|_{L_R}\delta\hat{G}(s,L_R) + \frac{G_{R0}^2}{2g_c\rho_f}\Big|_{L_R}\delta\hat{\Phi}_R(L_R)\right\} \quad (2.28)$$

Expressing the perturbed parameters in Equation (2.28) in terms of the external forcing functions, the pressure drop perturbation in the riser is given as the form of

$$\delta(\Delta\hat{P}_R)=R_1\delta j_i+\sum_{j=1}^{K}R_{2,j}\delta\hat{q}_j'' \quad (2.29)$$

II. 4. 3. Downcomer

The saturated water from the separator will be mixed with the subcooled water and enter the downcomer. The flow rate pertubation of the saturated water induces a downcomer water level perturbation, $\delta\hat{L}_D$.

The perturbed and Laplace-transformed mass continuity equation yields

$$\delta\hat{L}_D=\frac{1}{\rho_f A_D s}\{\delta\hat{W}_s-\rho_f A_{x-s}\delta j_i\} \quad (2.30)$$

When the complete phase separation is assumed in the seperator,

$$W_{sw}=(1-\langle x\rangle^{\text{out}})A_R G_R^{\text{out}}. \quad (2.31)$$

Perturbing and Laplace-transforming Equation (2.31), the mass flow rate perturbation can be expressed in terms of the external forcing functions. From the perturbed momentum equation with the moving boundary, $\delta\hat{L}_D$, the pressure drop perturbation in this region becomes

$$\delta(\Delta\hat{P}_{sw})_{DC}=\left(\frac{L_D s}{g_c A_D}+\frac{f_D L_D W_{\text{swo}}}{g_c D_{HD}A_D^2\rho_f}\right)\delta\hat{W}_{\text{sw}} + \left(\frac{f_D W_{\text{swo}}^2}{2g_c D_{HD}A_D^2\rho f}-\frac{g}{g_c}\rho_f\right)\delta\hat{L}_D \quad (2.32)$$

Then, $\delta(\Delta\hat{P}_{DC})$ can be expressed in terms of the external forcing functions, as the form of

$$\delta(\Delta\hat{P}_{DC})=Q_1\delta\hat{j}_i+\sum_{j=1}^{K}Q_{2,j}\delta\hat{q}_j'' \quad (2.33)$$

Next below the feedwater junction, the saturated water is mixed with the feedwater and becomes the subcooled liquid. Thus the pressure drop perturbation through the downcomer can be calculated from the single-phase perturbed momentum equation and has the form of

$$\delta(\Delta P_1)=T_1(s)\delta\hat{j}_i \quad (2.34)$$

II. 5. Frequency Domain Stability Analysis

In the evaluation of a large linear system, the traditional approach is the frequency domain technique. Thus the simple block diagram for a feedback control system is shown as

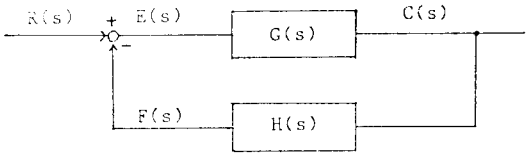

The closed loop transfer function becomes

$$\frac{C(s)}{R(s)}=\frac{G(s)}{1+G(s)H(s)}, \quad (2.35)$$

where $G(s)$ is the so-called forward loop transfer function and $H(s)$ is the feedback loop transfer function. Various methods are present to assess stability of a system. In this study, the Nyquist criterion is employed.[8]. In order to determine the proximity of the GH locus to the stability point, $(-1, 0)$, which is a measure of the relative stability of the system, a Nyquist plot is drawn, which consitst of the locus of the gain and the phase angle at different angular frequencies (ω). From this diagram, the gain and phase stability margins are determined.

These two factors are the measure of system relative stability.

Density-wave instability phenomenon are based on the constant pressure drop boundary condition. Thus, for the recirculation loop, the boundary condition will be

$$\delta(\Delta\hat{P}_{1\phi})_{loop}+\delta(\Delta\hat{P}_{2\phi})_{loop}=0.$$

By inserting the appropriate transfer functions described in the previous sections into this boundary condition, the open loop transfer function,

$$G(s)H(s)=-\frac{\delta\hat{j}_{i,F}}{\delta\hat{j}_{i,t}}=\frac{\Pi_1(s)+R_1(s)}{\Gamma_1(s)+T_1(s)+Q_1(s)}$$

can be obtained.

With this transfer function the stability analysis is carried out by using the Nyquist criterion.

III. Application and Results

III. 1. Program application

A computer implementation of this study, SASG, has been developed to analyze the instability in the recirculating loop of UTSG in the frequency domain. The SASG program can produce Nyquist plots corresponding to the external perturbation of the secondary side inlet velocity. The detailed models for the thermal-hydraulics of UTSG have been discussed in the previous parts of this paper.

Using this model, the stability analysis of the UTSG of Kori-Unit 1 has been performed with the input parameters summarized in Table 3. 1. The results from the SASG code demonstrates that this steam generator is stable against the density-wave oscillation type flow instability.

III. 2 Parametric study

Using the SASG program, the effects of various thermal hydraulic system parameters on the flow instability in the recirculation loop of UTSG were investigated. These parameters are the inlet velocity, the inlet subcooling, the inlet and riser outlet restriction, the local loss due to spacers, and the phasic slip. The operating conditions for the reference case are summarized in Table 3. 1.

Table 3.1. Operating Conditions of Reference Test

Primary side flow rate (lb/hr)	33.85×10^6
Primary side inlet temperature(F)	606.9
Primary side outlet temperature(F)	541.0
Primary side pressure(psia)	2250
Feed water flow rate(lb/hr)	3.775×10^6
Feed water temperature(F)	434
Steam flow rate(lb/hr)	3.775×10^6
Steam temperature(F)	518.9
Steam pressure(psia)	805
Recirculation ratio	3.25
Heat transfer area(ft^2)	51,500
Number of U-tubes	3388
U-tube outer diameter(in)	0.875
Tube wall thickness(in)	0.050
Density of tube material(lb/ft^3)	489.01
Specific heat of tube material(Btu/lb-F)	0.1098
Thermal conductivity of tube material (Btu/ft-hr-F)	10.3
Unheated riser length(ft)	7.285
Cross-sectional area of the unheated riser(ft^2)	101.917
Hydraulic diameter of the unheated riser(ft)	11.392
Downcomer flow area(ft^2)	8.112
Downcomer length(ft)	39.3945
Hydraulic diameter of downcomer(ft)	2.66
Loss coefficient of the heated section inlet	27.8
Loss coefficient of the riser outlet	4.1
Total number of spacers	7
Local loss coefficients of spacers	1.6

(1) The effect of inlet velocity

As the inlet velocity increases, the void fration decreases, and the single-phase length increases. Thus, as shown in Figure 3. 1, an increase in the inlet velocity stabilizes the system.

(2) The effect of inlet subcolling

The effect of the inlet subcooling on the stability is known not to be straight-forward, but dependent on the initial operating condition.[8]

At large subcooling, the effect of an increase is to stabilize the system. However, at smaller subcooling, an increase of the inlet subcooling destabilizes the system. In this parametric study,

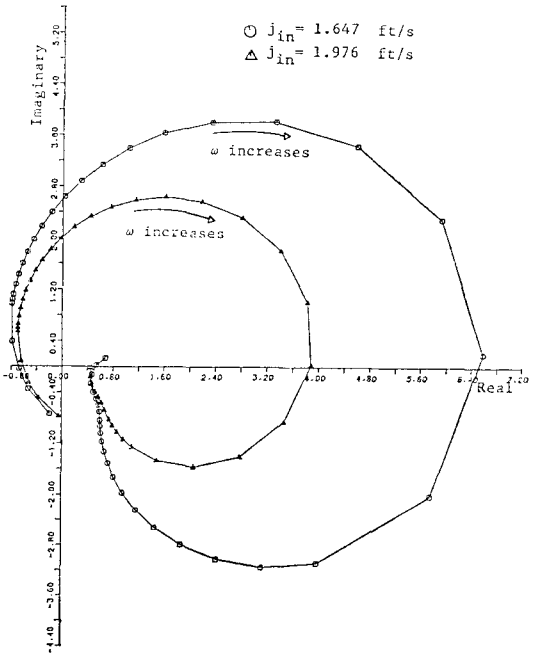

Fig. 3.1. The Effect of Inlet VelocityFig.

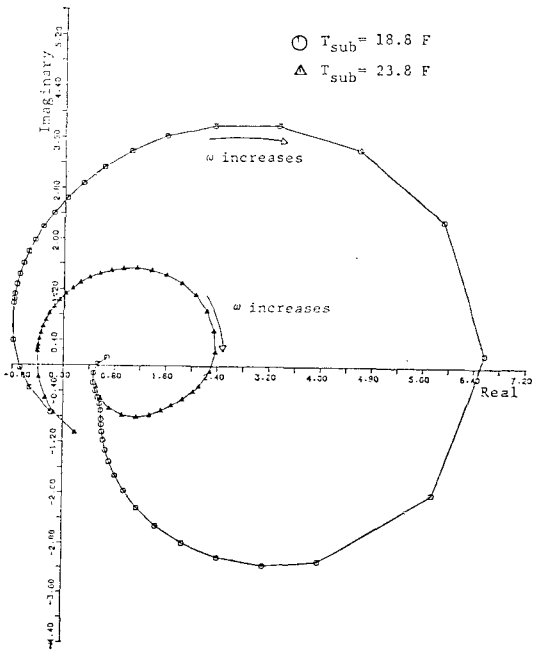

3.2. The Effect of Inlet Subcooling

the inlet subcooling is relatively large, ΔT_{sub}= 18°F, and thus an increase in the subcooling stabilized the system as shown in Figure 3.2.

(3) The effect of the heated section inlet restriction

An inlet restriction increase the single-phase pressure loss, which is in-phase with the inlet flow perturbation. Hence an increase of the inlet restriction has the stabilizing effect as shown in Figure 3.3.

(4) The effect of the riser outlet restriction

A restriction at the riser exit increases the two-phase exit loss, which is out-of-phase with the inlet flow perturbation. Thus, as shown in Figure 3.4, an increase in the exit restriction reduces the flow stability margin.

(5) The effect of spacers

Spacers located in the single and the two-phase region have similar relative effects as do inlet and outlet restrictions. Typically, an UTSG has 7 spacers which are equally spaced along the heated section. Since more of these spacers are in the two-phase region, they tend to destabilize

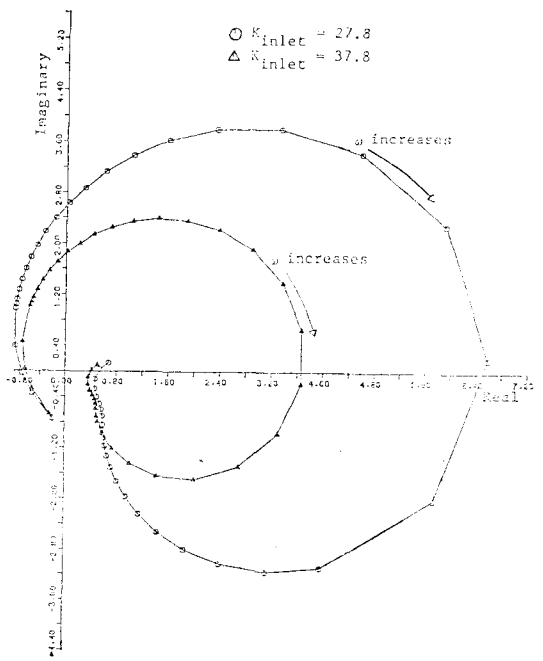

Fig. 3.3. The Effect of Inlet Restriction

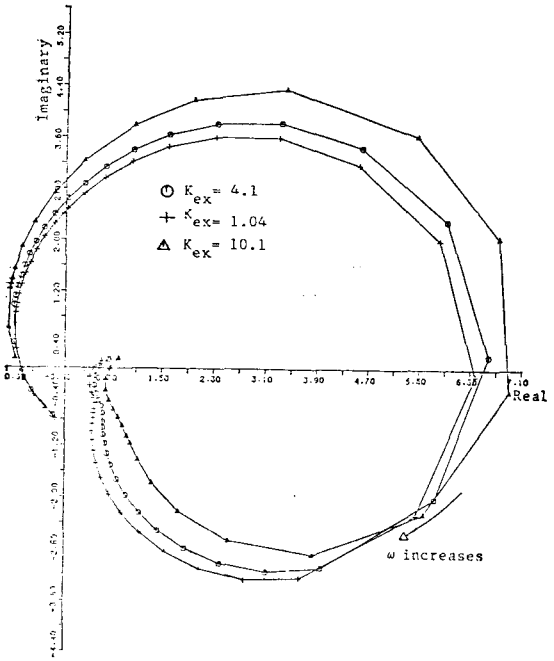

Fig. 3.4. The Effect of Riser Outlet Restriction

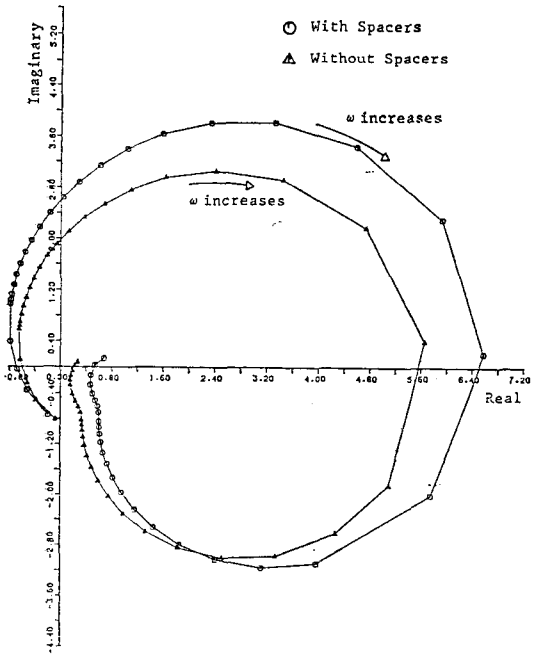

Fig. 3.5. The Effect of Spacer

the system, as shown in Figure 3.5.

(6) The effect of phasic slip

Since the phasic slip decreases the transport time of a density-wave through the loop, as well as the heated section void fraction, and thus the two-phase frictional and momentum pressure drop, the slip flow model makes the system more stable than the homogeneous flow assumption as shown in Figure 3.6.

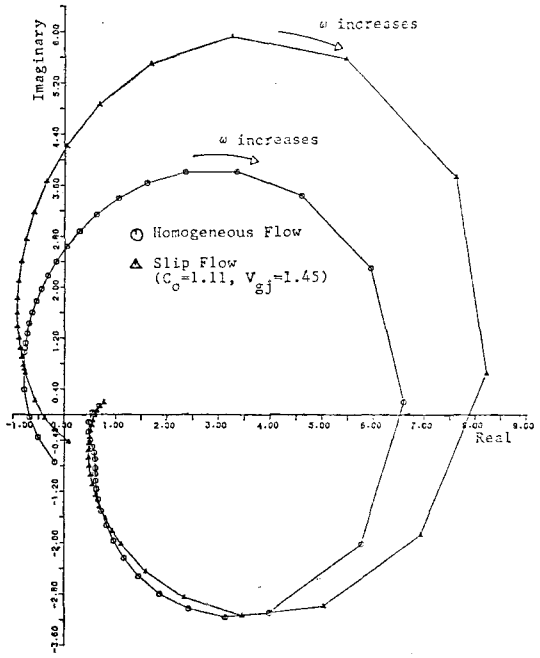

Fig. 3.6 The Effect of Slip

IV. Discussion and Conclusions

A state-of-the-art one-dimensional thermal-hydraulic model was developed to more accurately obtain the stability margin of a recirculating loop in the UTSG. This model, called SASG, accounts for phasic slip, arbitrary space time dependent heat flux distribution, distributed heated wall dynamics and an analytical model for each component in the loop.

This model has been applied to the stability analysis and the parametric study of the UTSG of Kori-Unit 1, which has revealed important factors influencing the steam generator stability margin. In conclusion, the parameters which improve the steam generator stability include

increases in: inlet restriction, inlet velocity, inlet subcooling, and phasic slip. Also a decrease in: exit restriction and the number of spacers in the two-phase region of the heated section, is stabilizing.

As the recommended future works, it is apparent that there is a real need for reliable out-of-plant and in-plant experimental stability data to test the accuracy of this model. In addition, it is clear that more of analysis are needed to develope a version of SASG which allows for the primary side heat flux perturbation as an external forcing function.

References

1. Lahey, R.T. Jr., and F.T. Moody, "The Thermal Hydraulics of a Boiling Water Nuclear Reactor," ANS Monograph(1977).
2. Ginox, J.J., "Two-Phase Flows and Heat Transfer with Application to Nuclear Reactor Design Problems," Hemisphere Publishing Corporation(1978).
3. G.C. Park, "The Development of NUFREQ-N; An Analytical Model For The Stability Analysis of Nuclear Coupled Density-Wave Oscillations in Boiling Water Nuclear Reactors," Ph. D. Thesis, RPI(1983).
4. J.C. Lee, et al., "TRANSG-01: A Computer Code for Transient Analysis of Nuclear Steam Generators," EPRI NP-3394-CCM, Electric Power Research Institute(1984).
5. J.C. Lee, et al., "Review of Transient Modeling of Steam Generator Units in Nuclear Power Plants," EPRI NP-1576, Electric Power Research Institute(1980).
6. J.P. Holman, "Heat Transfer," McGraw-Hill Inc. (1981).
7. Richard C. Dorf, "Modern Control Systems," Addison-Wesley Publishing Company(1974).
8. Neal, L.G. and S.M. Zivi, "A Comparative Study of Analytical Models and Experimental Data," STL 372-14, Vol. 1(1965).